Electronic Supplementary Material (ESI) for Journal of Materials Chemistry A.

Supporting Information

for

Multifunctional Fluorescent Chalcogenide hybrid nanodots ($MoSe_2$:CdS and WSe_2:CdS): As electro catalyst (for oxygen reduction/oxygen evolution reactions) and sensing probe for lead

Paramita Karfa,[a] Rashmi Madhuri,[a,*] Prashant K. Sharma[b]

[a]Department of Applied Chemistry, Indian Institute of Technology (Indian School of Mines),
Dhanbad, Jharkhand 826 004, INDIA

[b]Functional Nanomaterials Research Laboratory, Department of Applied Physics,
Indian Institute of Technology (Indian School of Mines),
Dhanbad, Jharkhand 826 004, INDIA

*Corresponding author: rshmmadhuri@gmail.com (R. Madhuri), Tel: +91 9471191640.

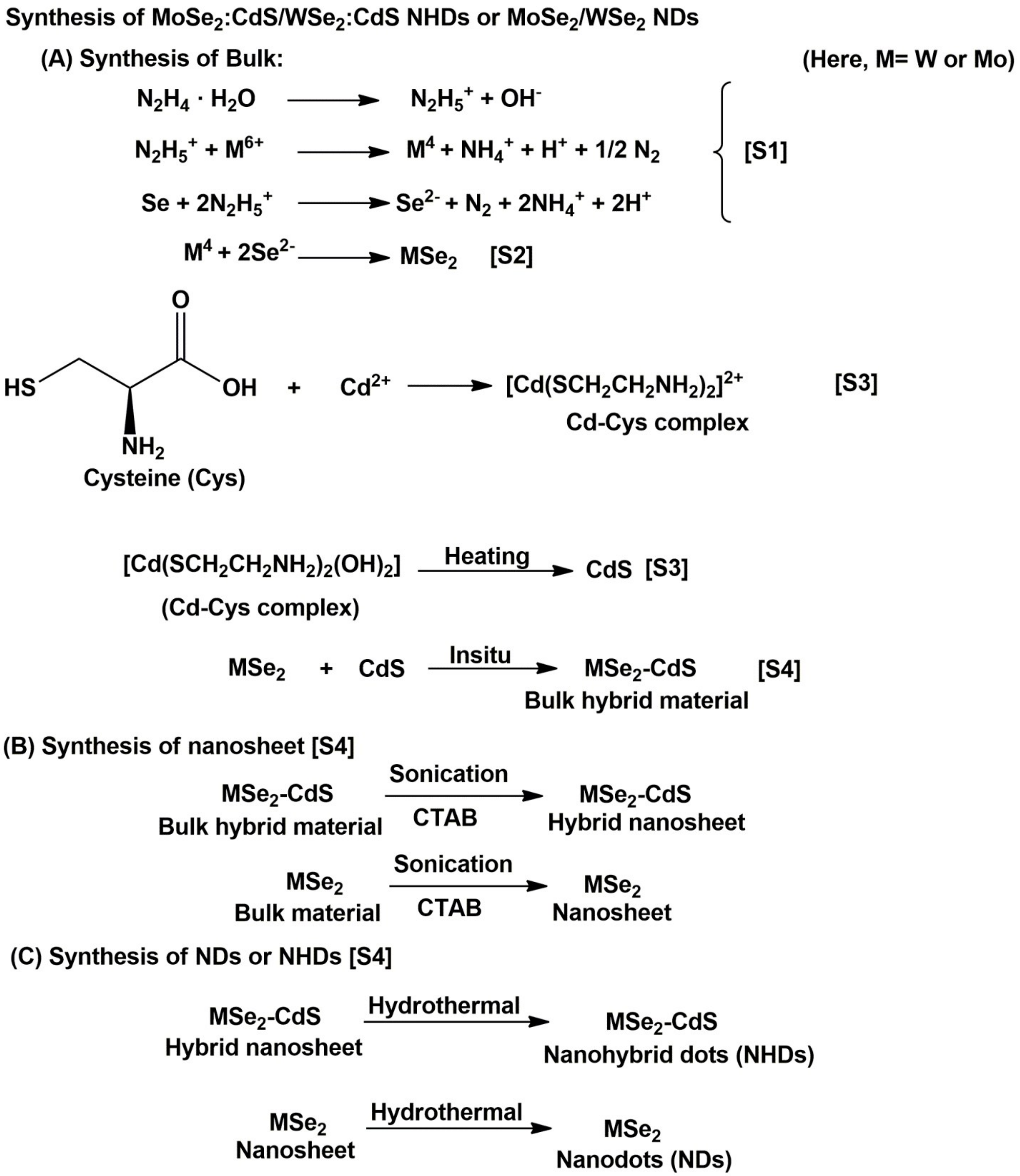

Scheme S1: Chemical reactions involved during synthesis of nanohybrid dots or nanodots from precursor compounds.

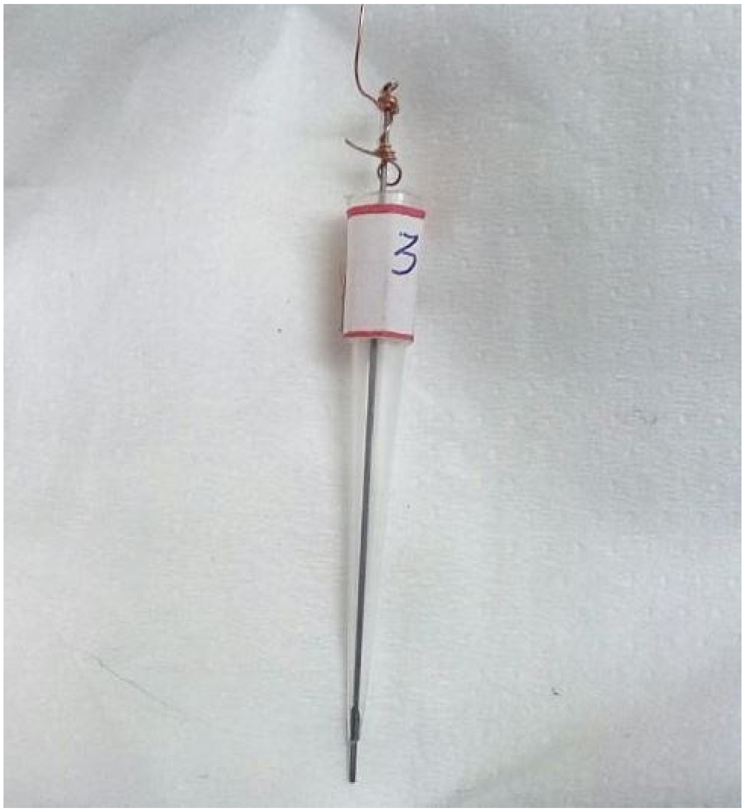

Figure S1: Camera picture of working electrode i.e. pencil graphite electrode (PGE) used in the electrochemical study.

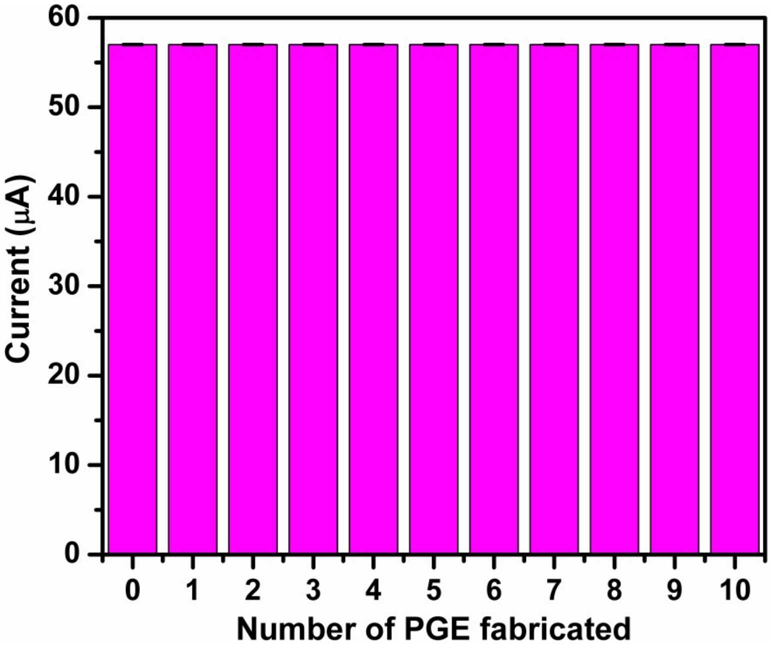

Figure S2: Reproducibility study during fabrication of pencil graphite electrodes (PGEs).

Table S1: Elemental composition of nanomaterials from XPS analysis.

S. N.	Nanomaterials	Elements (%)				
		Mo	W	Se	Cd	S
1.	$MoSe_2$:CdS Bulk	25.1	-	49.2	13.0	12.7
2.	$MoSe_2$:CdS Nanosheet	25.2	-	49.2	12.1	12.5
3.	$MoSe_2$:CdS NDs	25.4	-	49.7	13.6	12.3
4.	$MoSe_2$:CdS NHDs	25.6	-	49.9	12.0	12.5
5.	WSe_2:CdS Bulk	-	24.8	48.9	13.4	12.9
6.	WSe_2:CdS Nanosheet	-	25.1	48.2	13.5	13.2
7.	WSe_2:CdS NDs	-	25.6	48.5	13.8	12.1
8.	WSe_2:CdS NHDs	-	24.9	48.9	13.4	12.8

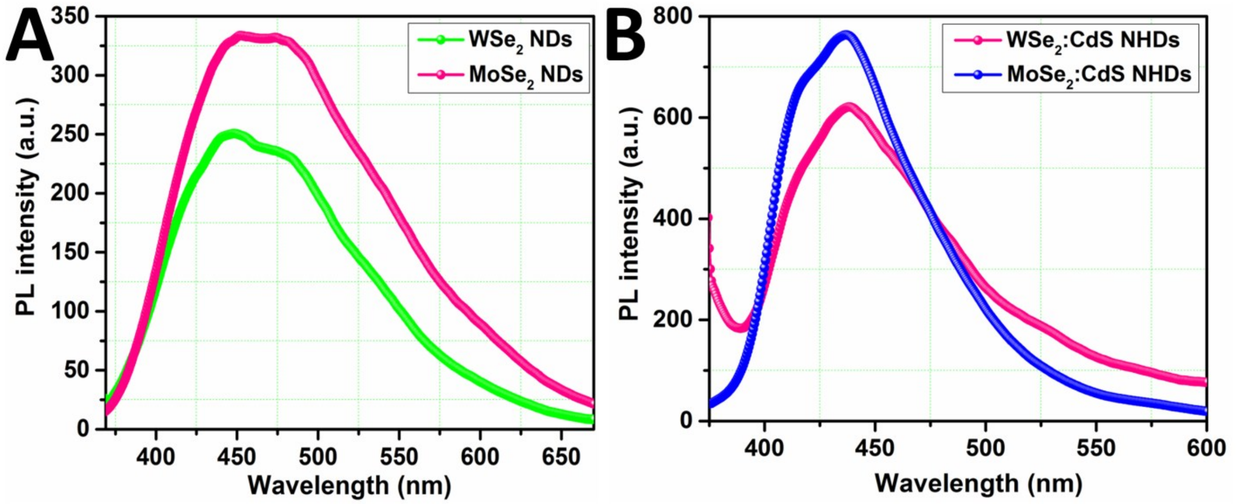

Figure S3: (A) PL emission spectra of WSe_2 and $MoSe_2$ nanodots (NDs) and (B) PL emission spectra of WSe_2:CdS and $MoSe_2$:CdS Nanohybrid dots (NHDs).

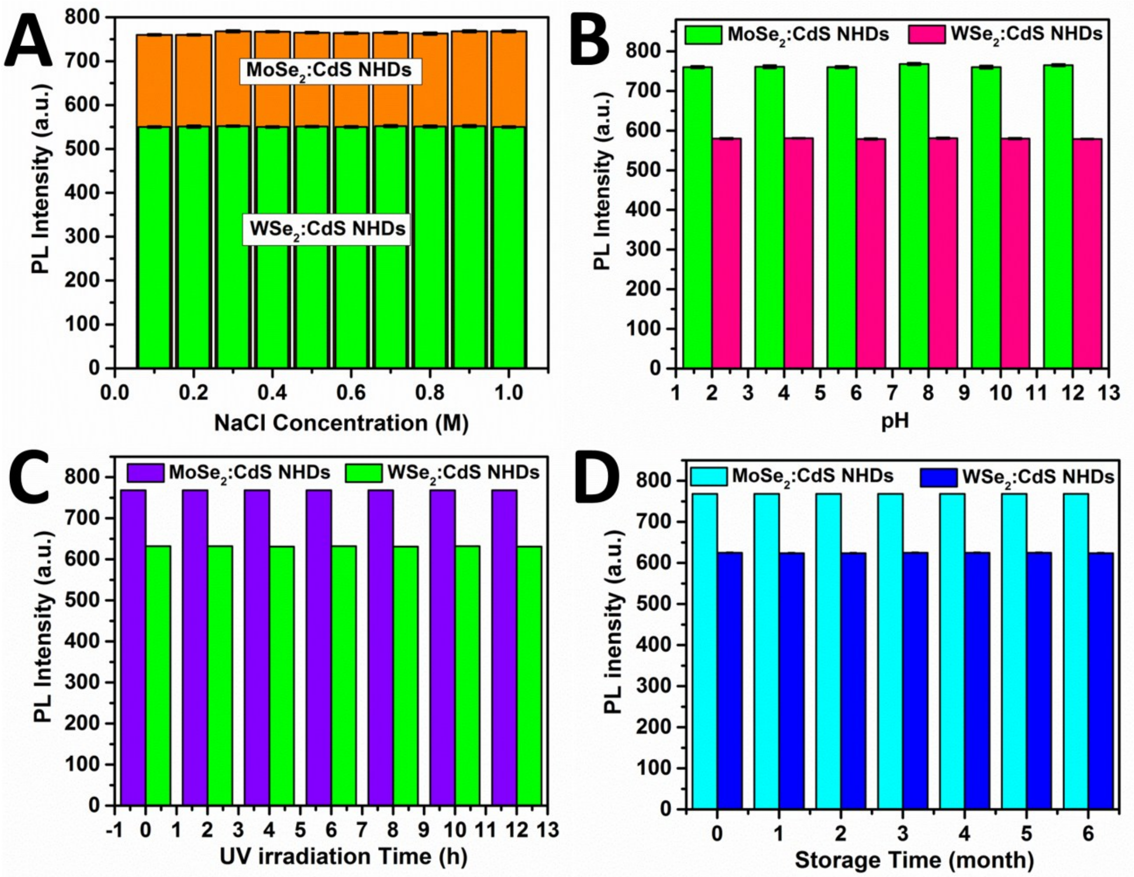

Figure S4: The stability of prepared NHDs against change in the (A) NaCl concentration, (B) pH, (C) UV irradiation time and (D) Storage time.

S1: Optimization of the electrochemical parameter

The electrochemical performance of the WSe_2:CdS for ORR and OER was optimized in different alkaline solution (0.05, 0.1, 0.5, 1.0 M KOH) in a standard three-electrode setup. In 0.1 (M) KOH lowest onset potential and low overpotential at 10 mA cm^{-2} is observed compared to other alkali medium value is on Linear sweep voltammetry (LSV) curves for OER, same change was observed for ORR in different alkali solution was recorded and shown in Figure S3 and S4. Furthermore, LSV runs were also taken by changing the loaded mass of the catalyst. We found that, initially the current density increased but decreased after the loading amount reached to 10.0 mg. This can be concluded due to the problem in mass transport, when the catalyst layer became relatively thick. Next is about the optimization of the scan rate, which was optimized in the range of 2.0 to 100.0 mV s^{-1}. It was found that at a scan rate of 5.0 mV s^{-1}, highest current density as well as better over potential value was observed for both ORR and OER.

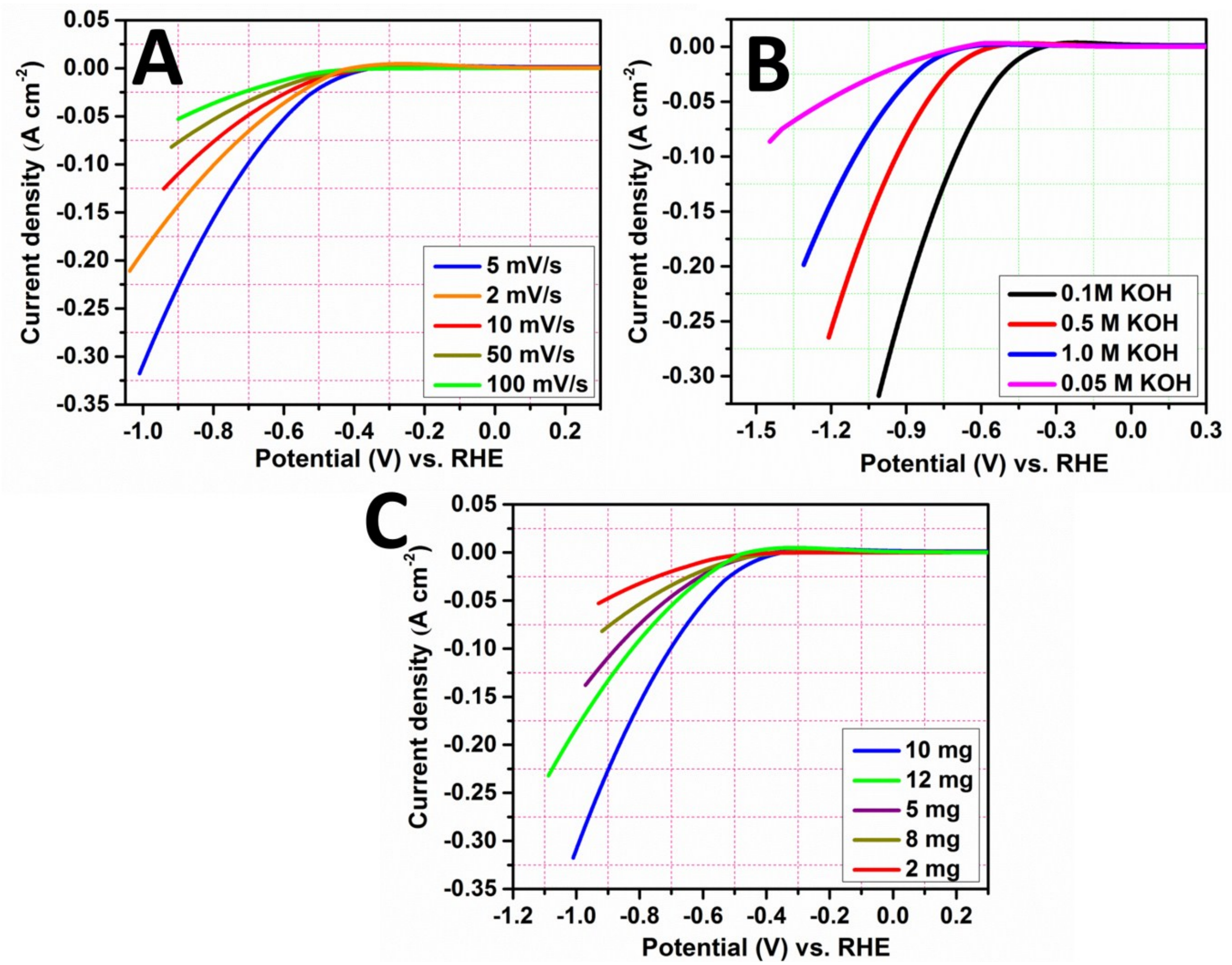

Figure S5: Optimization of analytical parameter for ORR: (A) Scan rate, (B) supporting electrolyte and (C) loading mass.

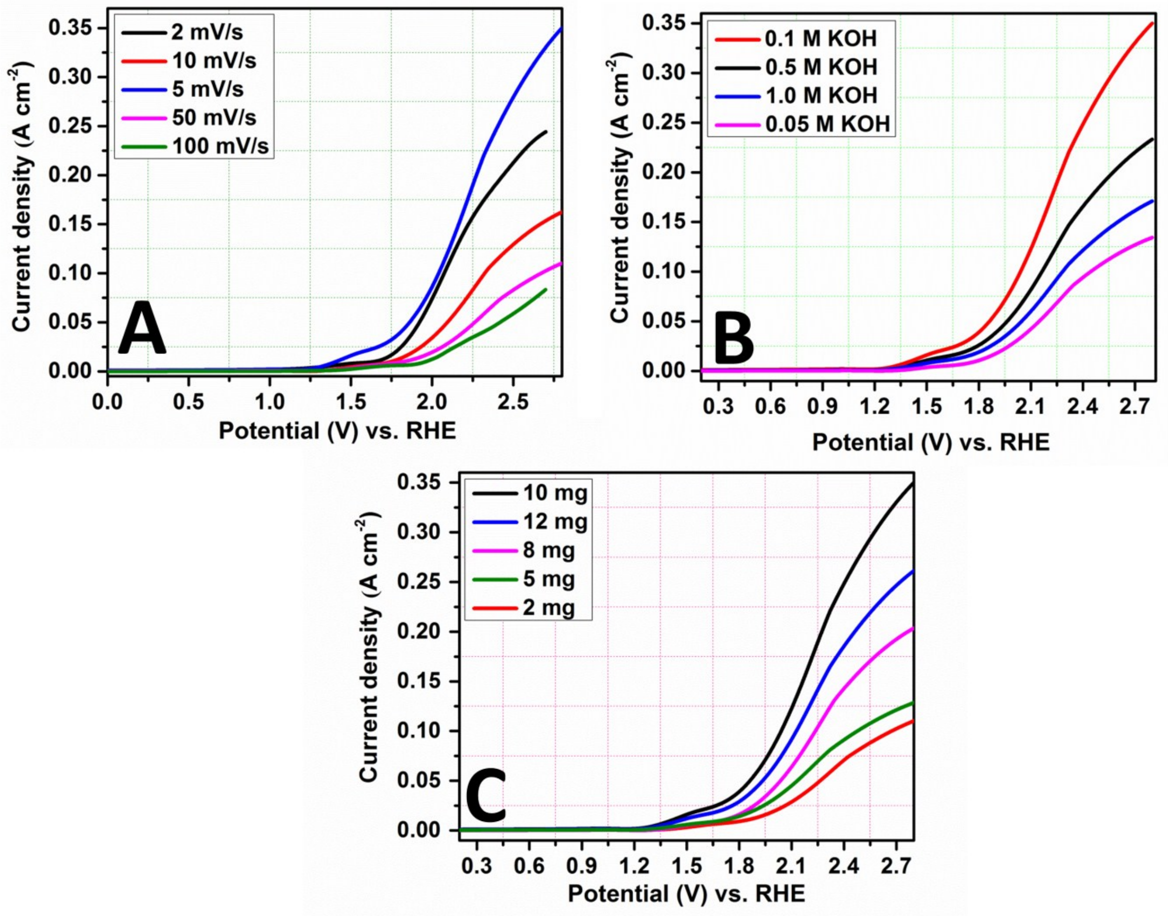

Figure S6: Optimization of analytical parameter for OER: (A) Scan rate, (B) supporting electrolyte and (C) loading mass.

A: ORR mechanism in alkaline medium:

1. $O_2 + H_2O + 2\ e^- \longrightarrow HO_2^- + OH^-$

2. $HO_2^- + H_2O + 2e^- \longrightarrow 3OH^-$

B: OER mechanism in alkaline medium:

$4\ OH^- \longrightarrow 2\ H_2O + O_2 + 4\ e^-$

Scheme S2: Probable reaction mechanism involved in OER and ORR taken from reference [S5].

S2. Blue bottle experiment

In order to confirm that the bubble formation at working electrode is due to the oxygen evolution, a blue bottle experiment was performed. For this, in the electrochemical cell containing KOH (1.0 M) and glucose, methylene blue was added. It was assumed that glucose will act as reducing agent and will change the colour of added methylene blue dye from blue to colourless leuco-methylene blue. Introduction or purging of external oxygen to this solution containing leuco-methylene blue will lead to the oxidation back to methylene blue, leading to regaining of its parent blue colour. When the dissolved oxygen has been fully consumed, methylene blue will slowly reduce back to its colourless form by the remaining glucose. Herein, when the electrochemical experiment was started, bubbles appear at the working electrode and therefore a blue color start appearing in the solution, due to conversion of leuco-methylene blue to methylene blue. We have recorded the video of the whole process, in which the 'light blue' colouration near to the electrode surface is clearly visible, owing to the oxidation of reduced methlyne blue, which confirms the formation of oxygen during the electrochemical process (SI-Video).

Further, UV- Vis spectroscopy is used to confirm the transformation of leuco-methylene blue to methylene blue, due to the presence of oxygen and shown in Figure S7. Initially, the UV Vis spectra of leuco-methylene blue solution shows a single peak at around 314 nm (peak marked as ‘a’), while in the presence of oxygen (the gas coming out from electrode), the peak intensity get decreases (from black, blue to red colour lines) and an increase in peak (peak marked ‘c’) intensity corresponds to methylene blue (664 nm) was observed. The reaction involved in the experiment was also shown in Scheme S3 [S6]. This clearly confirms the production of oxygen gas from the electrochemical set up.

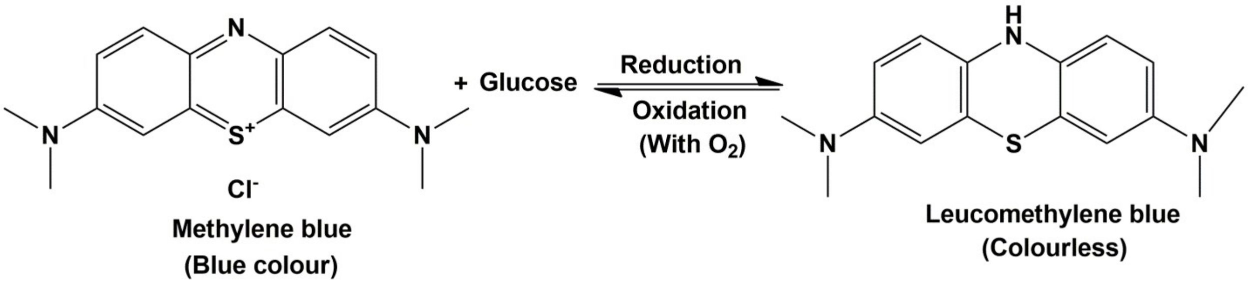

Scheme S3: Reaction mechanism involved in color change of methylene blue [S6].

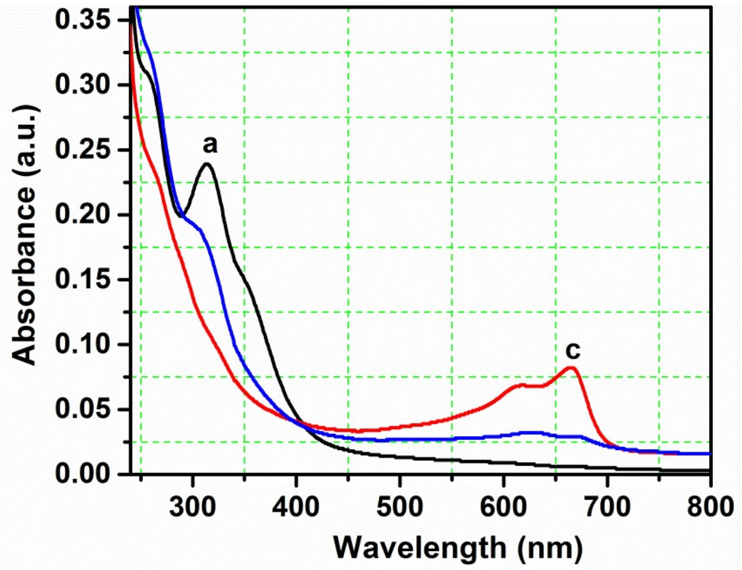

Figure S7: UV–Vis spectra of leuco-MB in presence of oxygen (the peak marked as 'a' corresponds to leuco- methylene blue and 'c' corresponds to methylene blue).

Table S2: Comparative study on differentially designed PGE.

S. N.	Electrode fabricated	CV current for ferricyanide (μA)	A (cm^2)	Roughness factor (R_f)
1.	Bare electrode	57	0.05	0.62
2.	WSe_2:CdS NHDs	346	0.31	3.85
3.	$MoSe_2$:CdS NHDs	284	0.26	3.23
4.	WSe_2 NDs	245	0.22	2.48
5.	$MoSe_2$ NDs	202	0.18	2.2
6.	WSe_2:CdS Nanosheet	144	0.13	1.6
7.	$MoSe_2$:CdS Nanosheet	126	0.11	1.4
8.	WSe_2:CdS Bulk	118	0.10	1.2
9.	$MoSe_2$:CdS Bulk	76	0.07	0.8

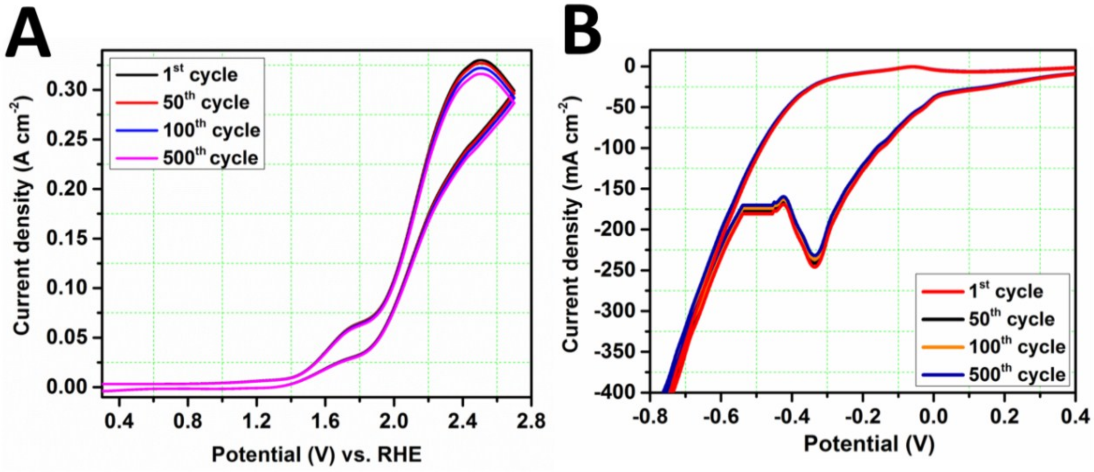

Figure S8: Stability study of prepared NHDs after multiple CV runs in different potential windows: (A) +0.4 to 2.6V (OER) and (B) +0.4 to -0.8V (ORR).

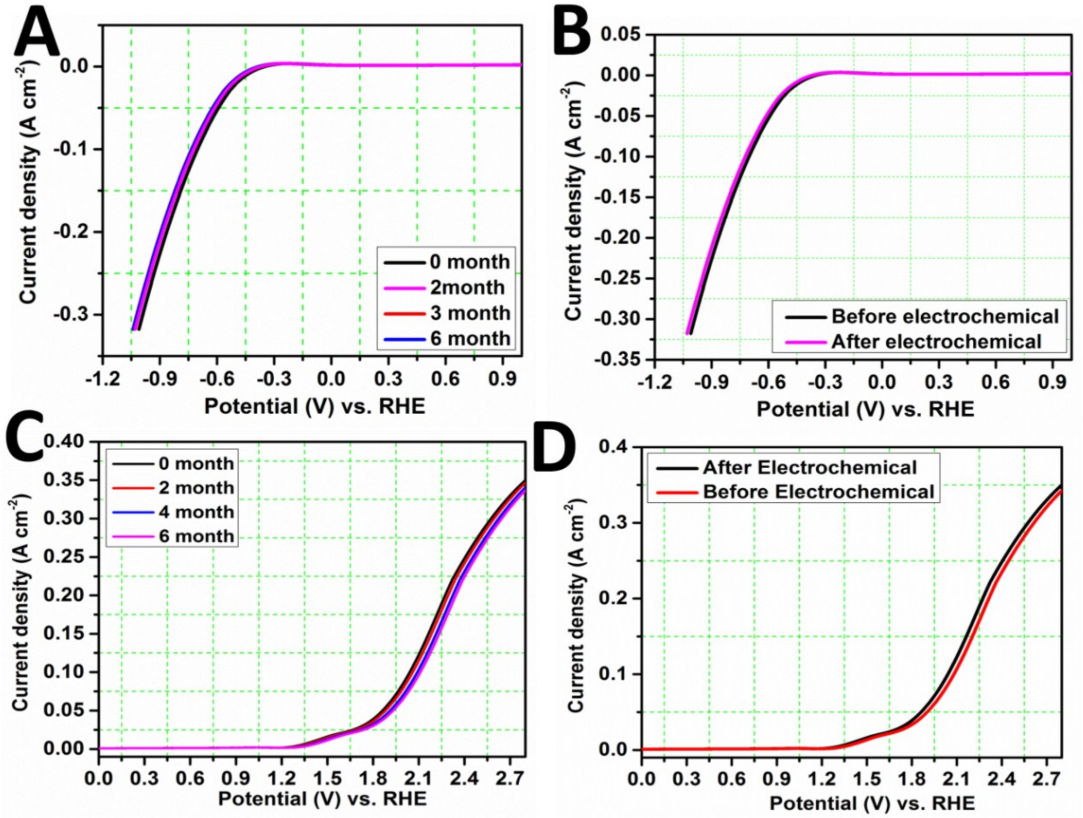

Figure S9: (A) The electrochemical storage stability of prepared NHDs tested by LSV runs after different storage duration and (B) Comparison of NHDs LSV runs, before and after electrochemical analysis, for ORR activity. (C) The electrochemical storage stability of prepared

NHDs tested by LSV runs after different storage duration and (D) Comparison of NHDs LSV runs, before and after electrochemical analysis, for OER activity.

Reference:

S1. P. Mulpur, T. M. Rattan and V. Kamisetti, *J. Nanosci.*, **2013,** Article ID 804290, 5 pages http://dx.doi.org/10.1155/2013/804290.

S2. P. P. Hankare, A. A. Patil, P. A. Chate, K. M. Garadkar, D. J. Sathe, A. H. Manikshete and I. S. Mulla, *J. Cryst. Growth*. 2008, **311**, 15–19.

S3. H. Gai, Y. Wu, L. wu, Z. wang, Y. Shi, M. Jing and K. Zou, *Appl. Phys. A*, 2008, **91**, 69–72.

S4. R. M. Clark, B. Carey, T. Daeneke, P. Atkin, M. Bhaskaran, K. Latham, I. S. Cole and K. Kalantar-zadeh, *Nanoscale,* 2015, **7**, 16763-16772.

S5. J. Duan, S. Chen, M. Jaroniec and S. Z. Qiao, *ACS catal*., 2015, **5**, 5207-5234.

S6. B.Z. Shakhashiri, *Chemical Demonstrations;* University of Wisconsin Press: Madison, 1985; **2**, 142.